

## Article

# The Calculation of Maximum Electric Field Intensity in Brain Tissue Stimulated by a Current Pulse through a Microcoil via Capacitive Coupling

Mohammed Alzahrani  and Bradley J. Roth \* 

Department of Physics, Oakland University, Rochester, MI 48309, USA; alzahrani@oakland.edu

\* Correspondence: roth@oakland.edu; Tel.: +1-(248)-375-2703

**Abstract:** The purpose of this paper is to calculate the maximum electric field in the brain tissue surrounding a microcoil. The microcoil is represented as a wire coupled capacitively to the surrounding tissue. For a 1 mA, 3 kHz current in the wire, the value of the electric field intensity in the tissue is approximately 4 mV/m. The intensity of the electric field is proportional to the frequency, the capacitance per unit area, and the square of the wire length. The electric field produced by this coil by electromagnetic induction is in the order of 0.002 mV/m. Therefore, the electric field produced by capacitive coupling is much greater than the electric field produced by induction. Methods to distinguish between capacitive and magnetic stimulation are discussed.

**Keywords:** magnetic stimulation; capacitive coupling; neural stimulation



**Citation:** Alzahrani, M.; Roth, B.J. The Calculation of Maximum Electric Field Intensity in Brain Tissue Stimulated by a Current Pulse through a Microcoil via Capacitive Coupling. *Appl. Sci.* **2024**, *14*, 2994. <https://doi.org/10.3390/app14072994>

Academic Editor: Piotr Gas

Received: 17 February 2024

Revised: 29 March 2024

Accepted: 1 April 2024

Published: 2 April 2024



**Copyright:** © 2024 by the authors. Licensee MDPI, Basel, Switzerland. This article is an open access article distributed under the terms and conditions of the Creative Commons Attribution (CC BY) license (<https://creativecommons.org/licenses/by/4.0/>).

## 1. Introduction

Magnetic stimulation therapy has become a highly effective treatment for many neurological conditions, such as depression [1]. In 1985, Dr. Anthony Barker invented transcranial magnetic stimulation, TMS, in which a current passes through a coil outside the head, with a strength of several kiloamps lasting a few hundred microseconds, and his device was able to stimulate the motor cortex in the brain [2]. This current causes a change in the magnetic field, which results in an induced electric field (electromagnetic induction) that can stimulate the nerves when it reaches the neuron's threshold for firing an action potential, helping and improving neurological symptoms such as depression and Alzheimer's disease [3–5]. Despite the widespread use of TMS therapy, it has poor spatial resolution, which makes it challenging to activate selectively the deeper targeted regions of the brain and achieve a focused stimulation [6–9].

Recently, microcoil technology has been a significant development in magnetic stimulation therapy [10–14]. (The term “microcoil” is often used, although these devices do not necessarily have a circular shape like a traditional “coil” but rather sometimes appear to be more like a bent wire.) Unlike traditional TMS, microcoils induce a highly localized and precise electric field, making it easier to stimulate specific brain regions [15]. The improvement in spatial resolution comes at the cost of implanting the microcoil, which makes its use more invasive. Nevertheless, for some applications the increase in spatial resolution may override the disadvantage of implantation. Researchers have made considerable progress in constructing microcoils with various sizes, shapes, and configurations. In 2012, Bonmassar et al. designed a microcoil with a radius of 500  $\mu\text{m}$  and a height of 1 mm, made from 21 turns of copper wire placed 300  $\mu\text{m}$  above the soma of an isolated ganglion cell [6]. When a few amps of current were passed through this microcoil, it produced a strong enough electric field to stimulate neurons effectively. Since then, other researchers have designed different microcoils requiring several amps of current and multiple coil turns to stimulate neurons [16,17]. This development of small, implantable microcoil technology has opened up new possibilities in treating neurological conditions, offering a new approach to

magnetic stimulation therapy. The critical concept in understanding microcoil stimulation is the electric field that it can produce. It can be affected by multiple factors, including the strength of the current and its frequency, the distance between the coil and the nerves, the number of coil turns, and the properties of the surrounding tissues.

In 2016, Lee et al. designed a single-turn microcoil and they were able to stimulate neurons with only a 40 mA current. They claimed that magnetic stimulation was the mechanism of this excitation [18]. Alzahrani and Roth were skeptical that magnetic stimulation was responsible for excitation because the induced electric field was too weak [19]. According to previous studies, the threshold for neuronal excitation is an electric field intensity of approximately 10 V/m [20,21]. (However, weaker fields, as low as 0.1 V/m, may alter the spontaneous firing rate in a neural network [22].) Alzahrani and Roth suggested that capacitive coupling may be a more likely mechanism than magnetic stimulation [19].

The primary purpose of this investigation is to calculate the electric field in the brain during neural stimulation using capacitive coupling. This paper presents an analysis of the electric field induced by capacitive coupling by utilizing the parameters from Lee et al.’s study [18]. We aim to provide a detailed calculation of the electric field generated by this method. Additionally, our study compares the results of the capacitive coupling analysis to the electric field expected during magnetic stimulation. With the increasing use of microcoil technologies in medical and therapeutic applications, the findings of this study provide insights into the mechanisms of exciting neurons.

## 2. Materials and Methods

We model the stimulating coil as a straight length of copper wire of radius  $a$  and length  $2L$ , surrounded by a tissue of radius  $b$  (we assume  $b \gg a$ ). The copper has conductivity  $\sigma_i$ , and the surrounding tissue has conductivity  $\sigma_e$ . The resistance per unit length of the wire is then  $r_i = 1/(\sigma_i \pi a^2)$  and that of the surrounding space is  $r_e = 1/(\sigma_e \pi b^2)$ . The two are coupled capacitively. The wire insulation has a capacitance per unit area  $C = \frac{\kappa \epsilon_0}{d}$ , determined by the dielectric constant of the insulator  $\kappa$  and its thickness  $d$ . We assume the resistance of the insulation is infinite. This model for the wire is essentially the same as the cable model for a nerve axon, except that we take the “membrane” conductance to be zero. Figure 1 illustrates the model.

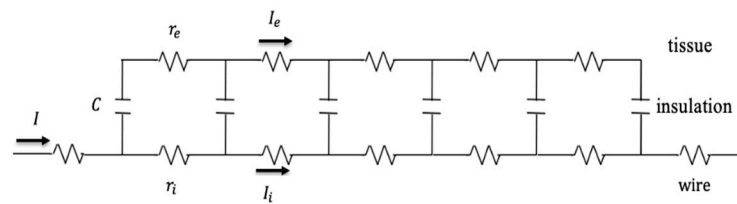


**Figure 1.** A model of a wire coupled to the surrounding tissue by a capacitance. The current in the wire is  $I_i$ , the wire resistance per unit length is  $r_i$ , the current in the tissue is  $I_e$ , the tissue resistance per unit length is  $r_e$ , the capacitance per unit area of the insulation is  $C$ , and the current applied to the wire at its ends is  $I$ .

Our analysis follows the traditional derivation of the cable equation [23]. The position along the cable is denoted by  $x$ , with  $x = 0$  at the center and  $x = \pm L$  at the ends. Time is denoted as  $t$ . To derive an equation governing the voltages in the wire,  $V_i$ , and in the surrounding tissue,  $V_e$ , we consider a section of the wire of length  $\Delta x$ . The wire current,  $I_i$ , entering this section from the left is  $I_i(x)$  and the current leaving this section on the right is  $I_i(x + \Delta x)$ . The current exiting the wire through the capacitance is  $C \partial(V_i - V_e)/\partial t$  times the wire’s surface area  $2\pi a \Delta x$ . Taking the limit as  $\Delta x$  goes to zero, this relationship becomes  $-\frac{\partial I_i}{\partial x} = 2\pi a C \frac{\partial(V_i - V_e)}{\partial t}$ . In the copper, the current and voltage are related by Ohm’s law,  $I_i = -\frac{1}{r_i} \frac{\partial V_i}{\partial x}$ , so this equation becomes  $\frac{1}{r_i} \frac{\partial^2 V_i}{\partial x^2} = 2\pi a C \frac{\partial(V_i - V_e)}{\partial t}$ . A similar relationship can be derived for the tissue space, but a minus sign is introduced because capacitive current

exiting the wire is entering the tissue. We can rearrange these expressions and define a diffusion constant as  $D = \frac{1}{2\pi a C(r_i+r_e)}$ , resulting in the pair of differential equations:

$$\frac{\partial}{\partial t}(V_i - V_e) = D \left( \frac{r_i + r_e}{r_i} \right) \frac{\partial^2 V_i}{\partial x^2} \text{ and } \frac{\partial}{\partial t}(V_i - V_e) = -D \left( \frac{r_i + r_e}{r_e} \right) \frac{\partial^2 V_e}{\partial x^2}, \tag{1}$$

Next, we introduce two new voltages—the voltage across the insulation,  $V$ , and a weighted average voltage,  $\psi$ —defined by

$$V = V_i - V_e \text{ and } \psi = V_i + \frac{r_i}{r_e} V_e, \tag{2}$$

which can be inverted to give  $V_i$  and  $V_e$  in terms of  $V$  and  $\psi$

$$V_i = \frac{r_e}{r_i + r_e} \left( \psi + \frac{r_i}{r_e} V \right) \text{ and } V_e = \frac{r_e}{r_i + r_e} (\psi - V). \tag{3}$$

We can use Equations (1) and (2) to show that  $V(x,t)$ , the voltage across the insulation, obeys the diffusion equation, and  $\psi(x, t)$ , a weighted average of the wire and tissue voltages, obeys a one-dimensional version of Laplace’s equation:

$$\frac{\partial V}{\partial t} = D \frac{\partial^2 V}{\partial x^2} \text{ and } \frac{\partial^2 \psi}{\partial x^2} = 0. \tag{4}$$

Our introduction of the diffusion constant earlier was motivated by its appearance in the diffusion equation for the voltage difference across the wire capacitance.

We assume a sinusoidal stimulus current (the system is driven by a current source, not a voltage source),  $I(t) = I_o \sin(\omega t)$ , where  $\omega = 2\pi f$  and  $f$  is the frequency. The diffusion time can be defined as  $L^2/D$  and is the same as the RC time constant of the wire: the resistance  $(r_i + r_e)L$  times the capacitance  $C2\pi aL$ .

For  $t < 0$ , the initial condition is  $V = \psi = 0$ . At the ends  $x = \pm L$ , all the current is in the wire and none is in the tissue, implying

$$\frac{\partial V_e}{\partial x} = 0 \text{ and } \frac{\partial V_i}{\partial x} = -I_o r_i \sin(\omega t). \tag{5}$$

In terms of  $V$  and  $\psi$ , these boundary conditions become

$$\frac{\partial V}{\partial x} = -r_i I_o \sin(\omega t) \text{ and } \frac{\partial \psi}{\partial x} = -r_i I_o \sin(\omega t). \tag{6}$$

The equation for  $\psi(x, t)$  in Equation (4) can be solved analytically:

$$\psi(x, t) = -r_i I_o \sin(\omega t)x. \tag{7}$$

The diffusion equation for  $V(x,t)$  in Equation (4) must be solved numerically [24]. The derivatives are approximated using finite differences with space step  $\Delta x$  and time step  $\Delta t$

$$V(x, t + \Delta t) = V(x, t) + D \frac{\Delta t}{\Delta x^2} [V(x + \Delta x, t) + V(x - \Delta x, t) - 2V(x, t)]. \tag{8}$$

The calculation must satisfy the stability criterion

$$\frac{4D\Delta t}{\Delta x^2} \leq 1. \tag{9}$$

The parameters we used in the calculation are given in Table 1, selected to approximately match those used experimentally by Lee et al. [18]. They imply  $D = 1.8 \text{ m}^2/\text{s}$ ,  $r_i = 850 \text{ } \Omega/\text{m}$ , and  $r_e = 320 \text{ M}\Omega/\text{m}$ . Clearly  $r_i \ll r_e$ , as would be expected. The DC

resistance of the coil is  $1.7 \Omega$ . The capacitance per unit area is  $C = 0.00011 \text{ F/m}^2$ . This is about a hundred times smaller than the capacitance of the cell membrane,  $0.01 \text{ F/m}^2$  or  $1 \mu\text{F/cm}^2$ , because the insulation thickness,  $300 \text{ nm}$ , is nearly a hundred times greater than the thickness of a cell membrane. The diffusion time is  $0.56 \mu\text{s}$ . In the calculation, we used  $\Delta x = 0.1 \text{ mm}$  and  $\Delta t = 0.001 \mu\text{s}$ , implying that the quantity on the left side of Equation (9) is  $0.72$  and that the calculation is stable.

**Table 1.** Parameters used in the calculation (from Lee et al. [18]).

Parameters	Definition	Value	Unit
$\kappa$	Insulation dielectric constant	3.8	-
$\sigma_e$	Tissue conductivity	0.1	$(\Omega\text{m})^{-1}$
$\sigma_i$	Wire conductivity	$60 \times 10^6$	$(\Omega\text{m})^{-1}$
$d$	Insulation thickness	300	nm
$a$	Wire radius	2.5	$\mu\text{m}$
$b$	Tissue radius	0.1	mm
$L$	Half the wire length	1	mm
$I_0$	Amplitude of applied current	1	mA
$f$	Frequency	3	kHz

Using a MATLAB (version R2022b) program, we calculated the electric field generated by the model shown in Figure 1. The current in the wire was  $1 \text{ mA}$  with a frequency of  $3 \text{ kHz}$ . The voltage in the wire  $V_i$  and the tissue  $V_e$  varied as a function of time and space, and we expressed this variation using the functions  $\psi$  and  $V$  in terms of  $V_i$  and  $V_e$ . After determining the values of  $\psi$  and  $V$  using the parameters outlined in Table 1, we could calculate the voltage along the wire  $V_i$  and the voltage in the tissue  $V_e$ . Finally, we calculated the electric field  $E$  in the tissue by taking the gradient of  $V_e$ . The MATLAB program used to perform the calculation is given in Supplementary Materials.

### 3. Results

When we calculate the voltages, we find that  $\psi$  and  $V$  are nearly the same in the wire and the tissue: they are both approximately linear in  $x$  (Figure 2), and both are nearly sinusoidal in time (Figure 3). This behavior occurs because the diffusion time ( $L^2/D = 0.56 \mu\text{s}$ ) is much less than the period of the applied current ( $333 \mu\text{s}$ ). The voltage difference between the ends of the wire,  $\Delta V_i$ , is nearly equal to  $\Delta\psi$  for  $r_e \gg r_i$ , so from Figure 2, we see that the voltage difference is about  $1.7 \text{ mV}$ . The voltage in the tissue,  $V_e$ , is approximately the difference between  $\psi$  and  $V$ , which is difficult to determine from Figures 2 and 3 but is not zero (Figure 4). It has a maximum amplitude at the ends of the coil and a maximum slope at the center. The magnitude of the electric field in the tissue is about  $4 \text{ mV/m}$  at  $x = 0$ .

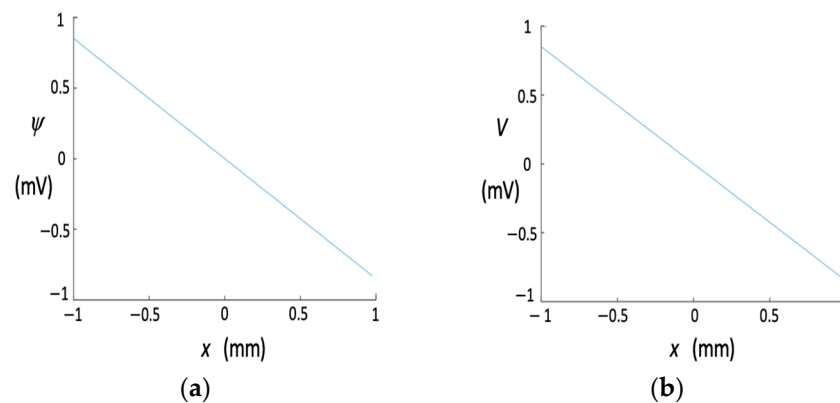


**Figure 2.** (a) The weighted average voltage  $\psi$  and (b) the voltage across the insulation  $V$  as functions of position  $x$  at time  $t = 83 \mu\text{s}$  (the time of the peak of the first phase of the sine wave).

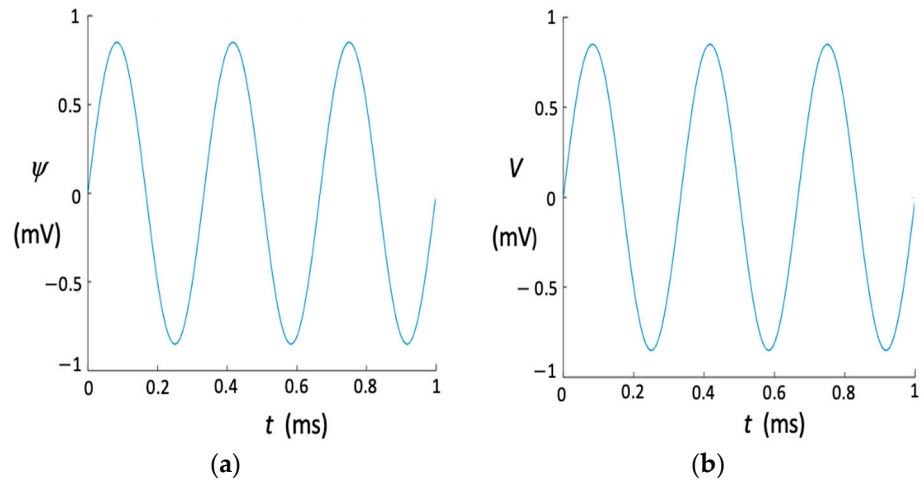


**Figure 3.** (a) The weighted average voltage  $\psi$  and (b) the voltage across the insulation  $V$  as functions of time  $t$  at position  $x = -10$  mm (the left end of the wire).

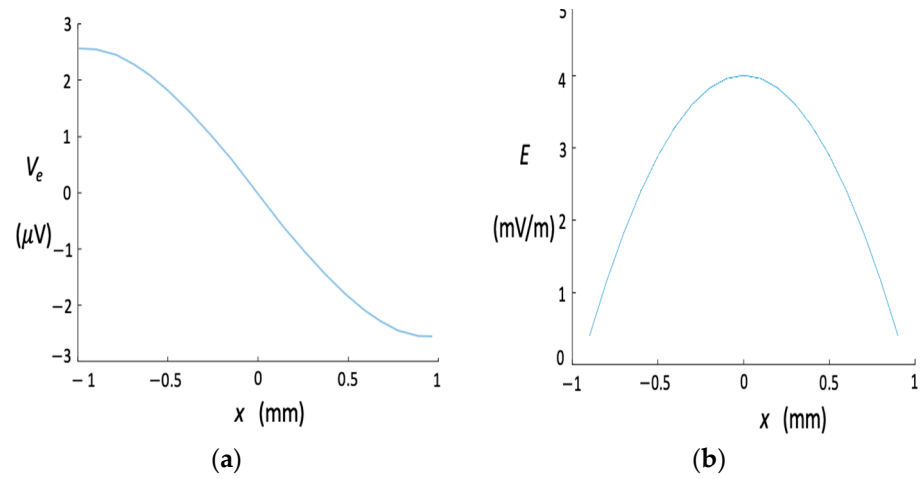


**Figure 4.** (a) The voltage in the tissue  $V_e$  and (b) the tissue electric field  $E$  as functions of position  $x$  at time  $t = 333$   $\mu$ s.

The time course for  $V_e$  and  $E$  (Figure 5) are approximately proportional to  $\cos(\omega t)$ . Therefore, the tissue electric field is 90 degrees out of phase with the coil current. Because the initial condition is  $V_e = 0$ , the tissue potential rises abruptly near  $t = 0$  (Figure 6). In about one microsecond (roughly the diffusion time) it reaches its asymptotic behavior.

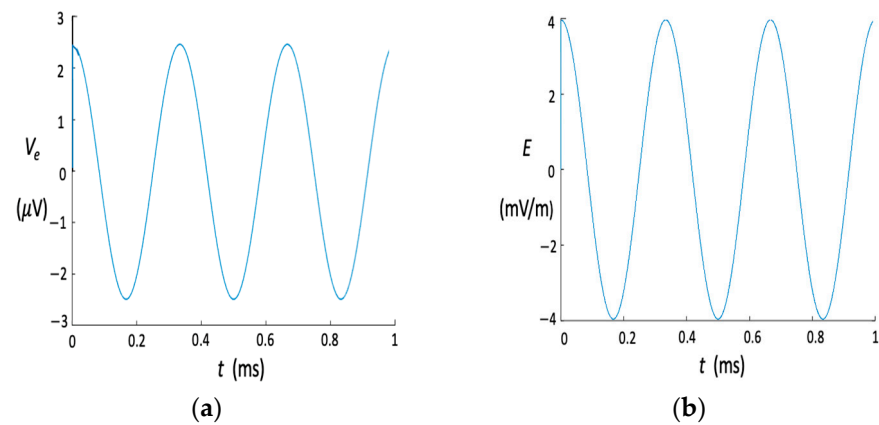


**Figure 5.** (a) The voltage in the tissue,  $V_e$ , at position  $x = -10$  mm and (b) the tissue electric field,  $E$ , at position  $x = 0$ , both as functions of time  $t$ .

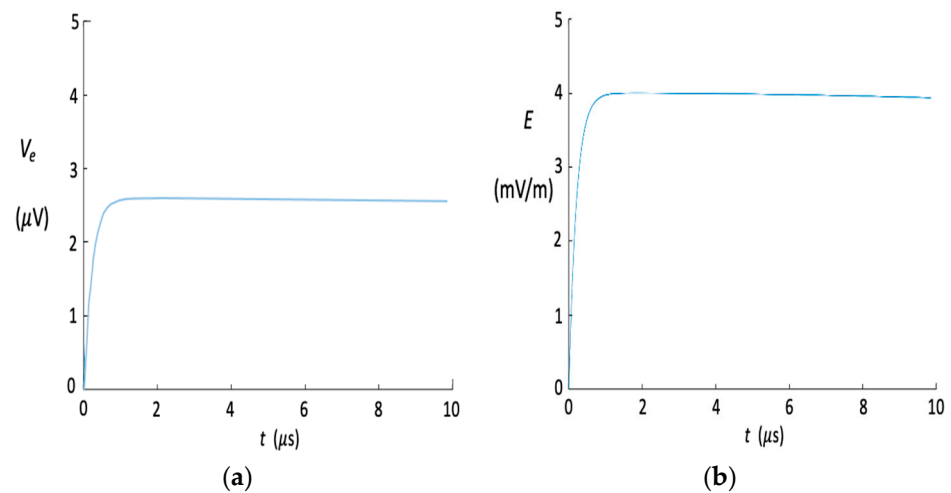


**Figure 6.** (a) The voltage in the tissue,  $V_e$ , at position  $x = -10$  mm and (b) the tissue electric field,  $E$ , at position  $x = 0$ , both as functions of time  $t$ . This is the same data as in Figure 5, but over a shorter range of times.

The voltage drop across the tissue is about 0.005 mV, compared to a drop of 1.7 mV in the wire. The tissue voltage drop, and therefore the tissue electric field, is so small because of the high resistance of the current path through the tissue (about 640,000  $\Omega$ ) compared to that through the wire (1.7  $\Omega$ ). Neither the tissue conductivity nor the radius of the cylindrical tissue space is known accurately, and the tissue conductivity may be heterogeneous [25]. Figure 7 shows the peak electric field strength as a function of the tissue resistance per unit length,  $r_e$ .

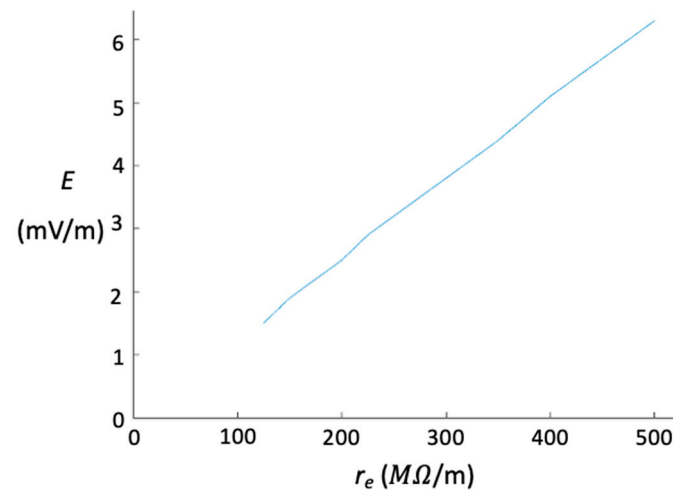


**Figure 7.** The peak tissue electric field intensity,  $E$ , as function of the tissue resistance per unit length,  $r_e$ .

Lee et al. [18] performed a test to determine if capacitive currents were important by passing a large transient current to burn a small portion of the coil, leaving an open circuit. We can simulate this experiment by dramatically increasing  $r_i$ . When we set  $r_i = 30$  M $\Omega$ /m, we found that the electric field was 143,385 mV/m.

The stability criterion defined earlier slows the numerical calculation because it implies a very small time step. We had to use a time step (0.001  $\mu$ s) that is more than 100,000 times shorter than the period of the stimulation current (333  $\mu$ s).

Except for a brief time when the stimulus first turns on (Figure 6), the electric field in the tissue follows a sinusoidal time course. Therefore, to a good approximation, we could calculate the electric field analytically for a sinusoidal current that extends over all time.

We assume  $V_e \ll V_i$  and  $r_i \ll r_e$ . In that case, Equation (3) implies that  $V_i = \psi$ ; the second expression in Equation (1) then becomes

$$\frac{\partial \psi}{\partial t} = -D \frac{\partial^2 V_e}{\partial x^2}. \tag{10}$$

Since  $\psi$  is known from Equation (7), we can simply integrate Equation (10) to obtain an approximate analytical expression for the tissue voltage

$$V_e \approx \frac{r_i}{D} I_0 \omega \cos(\omega t) \left[ \frac{x^3}{6} - \frac{L^2 x}{2} \right], \tag{11}$$

and for the tissue electric field

$$E \approx \frac{r_i}{D} I_0 \omega \cos(\omega t) \left[ \frac{L^2}{2} - \frac{x^2}{2} \right]. \tag{12}$$

At  $x = 0$ , the amplitude of the electric field is thus  $\frac{L^2 r_i \omega}{2D} I_0$ , which agrees fairly well with Figure 5. We have performed several numerical simulations and found them to be consistent with this approximate analytical analysis. For instance, our calculations indicate that the electric field intensity in the tissue is proportional to the frequency. Figure 7 indicates the electric field is proportional to the tissue resistance per unit length, which follows from the factor of the diffusion constant in the denominator of our analytical solution.

In traditional transcranial magnetic stimulation, the current through the coil is not sinusoidal but instead is delivered as a pulse. We have performed a simulation using a current pulse through the wire with an amplitude of 1 mA, a rise time of 10  $\mu$ s, and a subsequent decay of about 1 ms (Figure 8). The electric field in the tissue rises abruptly to a peak of 0.7  $\mu$ s after the pulse begins, and then decays and changes sign, but with a low amplitude. The peak amplitude of the electric field is about 50 mV/m, which is somewhat larger than found during a simulation with a sinusoidal current because of the abrupt rise in the pulse. In other words, during a Fourier analysis, frequencies greater than 3 kHz contribute to the rapid rise of the current waveform.

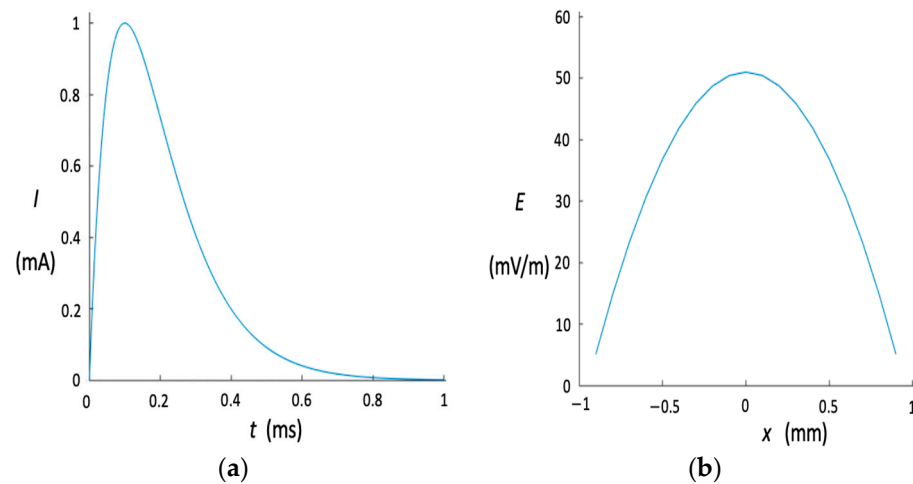


**Figure 8.** (a) The current,  $I$ , applied to the wire as a function of time,  $t$ , and (b) the peak tissue electric field intensity,  $E$ , as a function of position,  $x$ , at time 0.7  $\mu$ s.

#### 4. Discussion

Capacitive effects are known to be important for stimulating electrodes [26]. Typically, such electrodes are either Faradaic (where a chemical reaction occurs at the interface between the wire and the tissue) or capacitive (where charging or discharging a charged double layer at the electrode surface allows the stimulating current to enter the tissue).

However, these electrodes typically connect the stimulating circuit to a grounded tissue space. In other words, the electrode capacitance is in series with the wire injecting the stimulating current, and a second grounded electrode is required to provide the return path for the current. Our case is different. The wire capacitance is distributed in parallel along the length of the wire. Capacitive current passes out of the wire at one end and returns back into the wire at the other end. In essence, one end of the wire acts as the cathode and the other end as the anode. This is a very different circuit than used when analyzing most stimulating electrodes; no separate ground electrode is required. Our model resembles, in fact, an undersea telegraph cable or an axon within a nerve more than the usual stimulating electrode.

This model shows that a wire passing a sinusoidal current with a frequency of 3 kHz and amplitude of 1 mA produces an electric field in the surrounding tissue of about 4 mV/m. This value of  $E$  is small compared to the value required for excitation of neurons in the brain. Hulse found that the transmembrane potential produced in a single neuron in an electric field of 10 V/m can polarize a neuron by 6 to 8 mV, implying that the threshold is in the order of 10 V/m, or 10,000 mV/m [20]. Our value of  $E$  is about 2500 less than this threshold. Therefore, the electric field induced by capacitive coupling for a 1 mA, 3 kHz current should be well below the strength needed for neural excitation. In their calculations, Lee et al. used a nominal value of 1 mA for the current, but in their experiments, they found thresholds in the order of 40 mA [18]. A current of 40 mA would increase our calculated electric field up to 160 mV/m, bringing the stimulus closer to the expected threshold, within a factor of about 60.

For long, straight axons, the “activating function”  $dE/dx$  is often used as the source of electrical stimulation rather than the electric field itself. However, in the brain where axons bend and terminate, the electric field is more appropriate. The differences between these mechanisms are discussed in detail in [27].

Lee et al. assumed the electric field in the tissue was caused by magnetic stimulation, and calculated its amplitude to be about 1000 mV/m [18]. However, using arguments like those presented by Alzahrani and Roth [19], the electric field produced by magnetic stimulation should be in the order of

$$E \approx \frac{\mu_0}{4\pi} \frac{dI}{dt} \approx \frac{\mu_0}{4\pi} I_0 2\pi f \quad (13)$$

where  $\mu_0$  is the permeability of free space ( $4\pi \times 10^{-7}$  V s/(A m)). For  $I_0 = 1$  mA and  $f = 3$  kHz,  $E$  should be in the order of 0.002 mV/m, which is nearly a factor of a million smaller than the value Lee et al. calculated. (We have no explanation for why their calculation gave such a large value because we do not have access to their computer code; the computer code for our magnetic stimulation calculation is given in [19].) In this case, the electric field from magnetic stimulation (0.002 mV/m) is more than a thousand times smaller than the electric field from capacitive coupling (4 mV/m), implying that capacitive coupling is the dominant mechanism. A more accurate calculation of the electric field arising during magnetic stimulation with a microcoil was performed by Alzahrani and Roth, and they found the electric field to be about 0.026 mV/m [19] at a distance just outside the coil insulation surface (0.3  $\mu$ m from the coil).

How could one distinguish experimentally a model based on capacitive coupling from one based on magnetic stimulation? (1) Both predict an electric field that is proportional to the frequency and the amplitude of the applied coil current and that is out of phase with the coil current. (2) Increasing the thickness of the insulation should decrease the capacitance, thereby increasing the diffusion constant and making capacitive stimulation even more difficult. Magnetic stimulation, on the other hand, should not be affected by the thickness of the insulation. (3) The electric field produced by capacitive stimulation is sensitive to the tissue resistance (Figure 7), but the electric field induced by magnetic stimulation is not. (4) If the wire were made from silver instead of copper, then  $r_i$  would be smaller. This would decrease the electric field via capacitive stimulation, but (assuming a

current source) this would not affect magnetic stimulation. (5) Increasing the wire gauge and thus decreasing the wire radius would increase  $r_i$ , which would increase the electric field caused by capacitive stimulation. There would be no effect of wire gauge during magnetic stimulation (again, assuming a current source). (6) The coil could be wound using more turns. This would have a complicated influence during capacitive stimulation because it would couple the individual windings capacitively. For magnetic stimulation, increasing the number of windings would increase the magnetic field (assuming a current source, so any changes in coil resistance or inductance do not affect the current). (7) Finally, the length of the coil leads ( $L$ ) would play a major role in capacitive stimulation, but less or no role during magnetic stimulation.

To examine some of these effects in more detail, if we make the wire thinner (decrease  $a$ ), we will increase  $r_i$ . But assuming that  $r_i$  is still much smaller than  $r_e$  and that we are driving the coil with a current source, increasing  $r_i$  should increase the magnitude of the tissue electric field, making it easier to stimulate. (Essentially, we increase the voltage drop along the wire.) For instance, when the resistance  $r_i$  becomes equal to the resistance of the tissue  $r_e$ , the peak of the electric field will be huge, about 1,500,000 mV/m. Note, however, that as we increase  $r_i$  while using a current source, the voltage produced by the source will grow. The current source must be powerful enough to produce such a voltage, otherwise letting  $r_i$  become large in our calculation is unrealistic. Nevertheless, the best way to stimulate neurons in the brain may be to use two electrodes, an anode and a cathode, with a gap ( $r_i = \infty$ ), as is often used in traditional electric stimulation [26].

Increasing the resistance of the tissue space,  $r_e$ , would decrease  $D$  and increase the electric field in the tissue (Figure 7). For instance, making  $r_e$  ten times larger,  $r_e = 3200 \text{ M}\Omega/\text{m}$ , would increase the electric field in the tissue to 40 mV/m. The radius of the cylinder of tissue,  $b$ , is the least well-known parameter in our model. A more accurate calculation would treat the tissue as a volume conductor and determine the distribution of the tissue voltage and electric field as a function of position. In this case, the average electric field in the tissue may be smaller than value we calculate, but its peak value adjacent to the insulation may be larger.

Our calculation only approximates the physical situation examined by Lee et al. [18]. Their coil was not a straight wire, but bent into a hairpin loop. We assumed the tissue exists in a 0.1 mm radius cylinder surrounding the wire, which is probably the most arbitrary assumption in our calculation. The electric field in the tissue is almost certainly not independent of distance from the wire, as we have assumed in our one-dimensional model. All these assumptions will impact the predicted electric field in the tissue. However, our main conclusion is that the electric field in the tissue is over one thousand times larger for capacitive stimulation than for magnetic stimulation. Our assumptions would need to account for three orders of magnitude of difference, but it is not clear if accounting for these assumptions would make the electric field larger or smaller.

The predicted electric field in the tissue is a factor of 60 less than what we would expect for the threshold for neural stimulation. Some combination of our assumptions and an error in the estimation of threshold as 10,000 mV/m might raise our predicted tissue electric field to threshold level. For instance, a hairpin loop may result in the tissue voltage drop occurring over the distance between the two parallel wires (0.1 mm) rather than over the length of the wire (2 mm), thereby raising the electric field in the tissue significantly. The evidence is convincing that Lee et al. were somehow exciting neurons in their experiment [18], but it is difficult to imagine what other mechanisms could be active besides capacitive coupling and magnetic stimulation.

Our model makes specific predictions about microcoil stimulation of the brain via capacitive coupling. We hope that our results will motivate experiments to test these predictions.

## 5. Conclusions

In summary, we predict an electric field in the tissue due to capacitive coupling of about 4 mV/m for a current of 1 mA and 3 kHz. The electric field produced by magnetic

stimulation would more than a thousand times less, in the order of 0.002 mV/m. Therefore, capacitive coupling must be the dominant mechanism for stimulation with a microcoil.

Capacitive coupling using 1 mA predicts a small electric field relative to what we would expect for the neural threshold (10,000 mV/m). Lee et al. observed that 40 mA currents were required for neural excitation, making our predicted electric field about 60 times smaller than the expected threshold [18]. Some combination of invalid assumptions in our calculation, such as the presence of a hairpin loop along the wire so the voltage drop occurs between the two parallel wires rather than along the entire wire length, and an overly conservative value for the neural threshold may explain the discrepancy between the predicted and expected excitation threshold. Regardless of the electric field strength relative to the excitation threshold, our primary prediction is that the electric field caused by capacitive coupling should be much larger than the electric field caused by magnetic stimulation.

**Supplementary Materials:** The following supporting information can be downloaded at: <https://www.mdpi.com/article/10.3390/app14072994/s1>, File S1: The MATLAB computer program.

**Author Contributions:** Conceptualization, B.J.R.; methodology, M.A.; software, M.A.; validation, M.A. and B.J.R.; writing—original draft preparation, M.A.; writing—review and editing, M.A. and B.J.R.; visualization, M.A.; supervision, B.J.R. All authors have read and agreed to the published version of the manuscript.

**Funding:** This research was supported in part by Taif University, Saudi Arabia.

**Institutional Review Board Statement:** Not applicable.

**Informed Consent Statement:** Not applicable.

**Data Availability Statement:** Data are contained within the article.

**Conflicts of Interest:** The authors declare no conflicts of interest.

## References

1. Rizvi, S.; Khan, A.M. Use of transcranial magnetic stimulation for depression. *Cureus* **2019**, *11*, e4736. [[CrossRef](#)] [[PubMed](#)]
2. Barker, A.T.; Jalinous, R.; Freeston, I.L. Non-invasive magnetic stimulation of human motor cortex. *Lancet* **1985**, *1*, 1106–1107. [[CrossRef](#)] [[PubMed](#)]
3. Koch, G.; Bonni, S.; Pellicciari, M.C.; Casula, E.P.; Mancini, M.; Esposito, R.; Ponzo, V.; Picazio, S.; Di Lorenzo, F.; Serra, L.; et al. Transcranial magnetic stimulation of the precuneus enhances memory and neural activity in prodromal Alzheimer's disease. *NeuroImage* **2018**, *169*, 302–311. [[CrossRef](#)] [[PubMed](#)]
4. Yesavage, J.A.; Fairchild, J.K.; Mi, Z.; Biswas, K.; Davis-Karim, A.; Phibbs, C.S.; Forman, S.D.; Thase, M.; Williams, L.M.; Etkin, A.; et al. VA Cooperative Studies Program Study Team. Effect of repetitive transcranial magnetic stimulation on treatment-resistant major depression in US veterans: A randomized clinical trial. *JAMA Psychiatry* **2018**, *75*, 884–893. [[CrossRef](#)] [[PubMed](#)]
5. Wyszowska, J.; Jankowska, M.; Gas, P. Electromagnetic fields and neurodegenerative diseases. *Przegląd Elektrotechniczny* **2019**, *95*, 129–133. [[CrossRef](#)]
6. Bonmassar, G.; Lee, S.W.; Freeman, D.K.; Polasek, M.; Fried, S.I.; Gale, J.T. Microscopic magnetic stimulation of neural tissue. *Nat. Commun.* **2012**, *3*, 921. [[CrossRef](#)] [[PubMed](#)]
7. Ridding, M.C.; Rothwell, J.C. Is there a future for therapeutic use of transcranial magnetic stimulation? *Nat. Rev. Neurosci.* **2007**, *8*, 559–567. [[CrossRef](#)]
8. Wagner, T.; Valero-Cabre, A.; Pascual-Leone, A. Noninvasive human brain stimulation. *Annu. Rev. Biomed. Eng.* **2007**, *9*, 527–565. [[CrossRef](#)]
9. Syrek, P.; Bărbulescu, R. Parametric curves to trace the TMS coils windings. In Proceedings of the 10th International Symposium on Advanced Topics in Electrical Engineering, Bucharest, Romania, 23–25 March 2017; pp. 386–391. Available online: <https://ieeexplore.ieee.org/document/7905069/> (accessed on 28 March 2024).
10. Liu, X.; Whalen, A.J.; Ryu, S.B.; Lee, S.W.; Fried, S.I.; Kim, K.; Cai, C.; Lauritzen, M.; Bertram, N.; Chang, B.; et al. MEMS micro-coils for magnetic neurostimulation. *Biosens. Bioelectron.* **2023**, *227*, 115143. [[CrossRef](#)]
11. Ye, H.; Hall, V.; Hende, J. Improving focality and consistency in micromagnetic stimulation. *Front. Comput. Neurosci.* **2023**, *17*, 1105505. [[CrossRef](#)]
12. Lee, K.J.; Park, B.; Jang, J.-W.; Kim, S. Magnetic stimulation of the sciatic nerve using an implantable high-inductance coil with low-intensity current. *J. Neural Eng.* **2023**, *20*, 036035. [[CrossRef](#)]
13. Tian, L.; Liu, Q.; Song, L.; Jin, Z.; Dong, L.; Zheng, Y. Design and optimization of resonance-based wireless power transmission for millimeter-sized planar square inductors micro-magnetic stimulation. *IEEE Trans. Instrum. Meas.* **2023**, *72*, 4009010. [[CrossRef](#)]

14. Jeong, H.; Deng, J.; Bonmassar, G. Planar figure-8 coils for ultra-focal and directional micromagnetic brain stimulation. *J. Vac. Sci. Technol. B* **2021**, *39*, 063202. [[CrossRef](#)] [[PubMed](#)]
15. Park, H.J.; Bonmassar, G.; Kaltenbach, J.A.; Machado, A.G.; Manzoor, N.F.; Gale, J.T. Activation of the central nervous system induced by micro-magnetic stimulation. *Nat. Commun.* **2013**, *4*, 2463. [[CrossRef](#)] [[PubMed](#)]
16. Park, H.J.; Kang, H.; Jo, J.; Chung, E.; Kim, S. Planar coil-based contact-mode magnetic stimulation: Synaptic responses in hippocampal slices and thermal considerations. *Sci. Rep.* **2018**, *8*, 13423. [[CrossRef](#)] [[PubMed](#)]
17. Yoshikawa, T.; Higuchi, H.; Furukawa, R.; Tateno, T. Temporal and spatial profiles of evoked activity induced by magnetic stimulation using millimeter-sized coils in the mouse auditory cortex in vivo. *Brain Res.* **2022**, *1796*, 148092. [[CrossRef](#)] [[PubMed](#)]
18. Lee, S.W.; Fallegger, F.; Casse, B.D.; Fried, S.I. Implantable microcoils for intracortical magnetic stimulation. *Sci. Adv.* **2016**, *2*, e1600889. [[CrossRef](#)]
19. Alzahrani, M.; Roth, B.J. The electric field induced by a microcoil during magnetic stimulation. *IEEE Trans. Biomed. Eng.* **2023**, *70*, 3260–3262. [[CrossRef](#)]
20. Hulse, L. A mathematical model for transmembrane potentials secondary to extracellular fields. In *Electroanaesthesia: Biomedical and Biophysical Studies*; Sances, A., Larson, S.J., Eds.; Academic Press: New York, NY, USA, 1975.
21. Tranchina, D.; Nicholson, C. A model for the polarization of neurons by extrinsically applied electric fields. *Biophys. J.* **1985**, *50*, 1139–1156. [[CrossRef](#)]
22. Francis, J.T.; Gluckman, B.J.; Schiff, S.J. Sensitivity of neurons to weak electric fields. *J. Neurosci.* **2003**, *23*, 7255–7261. [[CrossRef](#)]
23. Wu, J.; Wikswo, J.P. Effects of bath resistance on action potentials in the squid giant axon: Myocardial implications. *Biophys. J.* **1997**, *73*, 2347–2358. [[CrossRef](#)]
24. Press, W.H.; Teukolsky, S.A.; Vetterling, W.T.; Flannery, B.P. *Numerical Recipes in Fortran*; Cambridge Univ. Press: Cambridge, UK, 1992.
25. Syrek, P. Uncertainty problem as illustrated by magnetotherapy. *ACES J.* **2019**, *34*, 1445–1452.
26. Cogan, S.F. Neural stimulation and recording electrodes. *Annu. Rev. Biomed. Eng.* **2008**, *10*, 275–309. [[CrossRef](#)]
27. Roth, B.J. Mechanisms for electrical stimulation of excitable tissue. *Crit. Rev. Biomed. Eng.* **1994**, *22*, 253–305.

**Disclaimer/Publisher's Note:** The statements, opinions and data contained in all publications are solely those of the individual author(s) and contributor(s) and not of MDPI and/or the editor(s). MDPI and/or the editor(s) disclaim responsibility for any injury to people or property resulting from any ideas, methods, instructions or products referred to in the content.